

## BUMP CEPHEIDS: THE MASS ANOMALY AS AN OPACITY EFFECT

SASTRI K. VEMURY\* AND RICHARD STOTHERS

Institute for Space Studies, NASA Goddard Space Flight Center

Received 1977 December 27; accepted 1978 April 25

### ABSTRACT

Nonlinear calculations of models for bump Cepheids indicate that most of the basic features of these stars can be reproduced well by models having normal to nearly normal evolutionary masses and normal helium abundances, if Carson's opacities are adopted. The trends of the properties of the models with various physical parameters are otherwise very similar to those obtained by other authors with the Los Alamos opacities (which have led to Cepheid masses of half the evolutionary masses). Difficulties with the resonance hypothesis of Simon and Schmidt as an explanation of the bump are discussed.

*Subject headings:* opacities — stars: Cepheids — stars: pulsation

### I. INTRODUCTION

Classical Cepheids in the intermediate period range (7–15 days) show a prominent secondary bump on their observed light and radial-velocity curves. Up to the present time, a satisfactory theoretical reproduction of this bump has been achieved only by making one of two drastic assumptions: (1) that the mass of a Cepheid is about half the mass expected from standard evolutionary theory without mass loss (Christy 1968, 1975; Stobie 1969*b*, *c*; Rodgers 1970; Fricke, Stobie, and Strittmatter 1971, 1972) or (2) that the composition of the outer layers of a Cepheid is anomalously helium-rich or metal-rich (Cox *et al.* 1977; Cox, Michaud, and Hodson 1978).

The opacities used in obtaining these model results were generated from various versions of the Los Alamos opacity code, beginning with the original work of Cox and Stewart (1965). In an interesting experiment, Fricke, Stobie, and Strittmatter (1971) demonstrated that an arbitrary scale-factor increase of the Cox-Stewart opacities would lead to a proportionate increase in the inferred masses of bump Cepheids. Using this result and knowing that Carson's (1976) independently generated opacities are, in the crucial second helium ionization zone, larger by a factor of  $\sim 2$  than the Cox-Stewart opacities, Carson and Stothers (1976) predicted that the mass anomaly for bump Cepheids could perhaps be made to disappear simply by adopting the newer opacities.

In order to verify this prediction, we calculated a number of nonlinear models with Carson's opacities. These models showed the predicted secondary bump for nearly normal evolutionary masses (Vemury and Stothers 1977). However, with the same opacities, Cox (1977) independently computed a model for  $6.4 M_{\odot}$  obeying the normal evolutionary mass-luminosity relation and did not find a bump. Nor was he later able to obtain a bump for a model of  $7 M_{\odot}$  in which we had reported a large one. We confirm

\* Same as V. K. Sastri.

that the particular model of  $6.4 M_{\odot}$  originally computed by Cox does not show a bump. Regarding the  $7 M_{\odot}$  model, Cox (1977) afterwards obtained a bump for this model at a larger velocity amplitude ( $64 \text{ km s}^{-1}$  as compared with his earlier  $46 \text{ km s}^{-1}$ ). But he still had reservations about the Carson opacities. Although the validity of these opacities has also been questioned by Merts (1977), who tried, unsuccessfully, to reproduce them, it is equally true that the Los Alamos opacities themselves have not been tested and verified by an independent group. Carson (1976) himself has stressed the care with which his hydrogen and helium opacities were calculated. In any case, Carson and we regard stellar applications as being probably the only available test of the opacities at present.

These various considerations have motivated our present calculation of a large number of nonlinear Cepheid models based on the Carson opacities. We have studied deep stellar envelopes having composition parameters  $(X, Y, Z) = (0.739, 0.240, 0.021)$  and undergoing radial pulsations in the fundamental mode. In § II the computer program is described, with various tests of the program made in § III. The new nonlinear results are presented in § IV. Some discussion and improvements of the linear results published previously (Carson and Stothers 1976) are described in § V. Our main conclusions are summarized in § VI.

### II. THE COMPUTER PROGRAM

Several computer programs have been written by different authors to solve the nonlinear equations of stellar pulsation at large amplitude. There are found to be variations in detail among the different results that have been obtained for ostensibly the same stellar model by different authors, but the main features of the luminosity and velocity curves, including the secondary bumps, seem to agree. Since the present code has been created independently of the previous

codes, it is appropriate to describe our own procedures, physical input data, and a few ideas on how to achieve a functional program that do not seem to have been published previously, at least in any detail.

#### a) *The Static Model and the Initial Model*

First, a static model of the stellar envelope is constructed by solving (with the use of step-by-step numerical integrations) the familiar differential equations governing the equilibrium structure of the star. The envelope model is characterized by the total stellar mass  $M$ , luminosity  $L$ , effective temperature  $T_e$ , and chemical composition parameters  $X$ ,  $Y$ ,  $Z$ . In addition, the boundary conditions, thermodynamic state relations, and opacities need to be supplied. The boundary conditions are taken to be those of Christy (1967). The state relations apply to a mixture of radiation and nondegenerate gas in various stages of ionization; all the Saha equations for hydrogen, helium, and a hypothetical, easily ionized metal are solved simultaneously at every layer of the model in which  $\log T < 5.50$  (at hotter layers the gas is assumed to be completely ionized). The opacities used are the Carson radiative opacities in logarithmic tabular form (with linear interpolation used between grid points) for  $\log T > 3.85$ , and Cox and Stewart's radiative opacities in Christy's (1966) analytic fitted form for  $\log T < 3.85$ ; the two sets of opacities are found to match nearly perfectly at  $\log T = 3.85$ , in regard to both the value and the gradient of the opacity. Convection is completely ignored in our models; the diffusion approximation is adopted for radiative transfer at all layers.

The static model envelope thus derived usually contains 1000 or more zones. For the nonlinear calculations, strict limitations of computer time require that the adopted number of zones be small. Therefore, about 40 zones are selected in the manner suggested by Christy (1967). The optically thin part of the envelope contains four or five zones, the narrow hydrogen ionization region has one or two, and the innermost zone is assigned to be near a radius fraction  $r/R$  of 0.10. From this coarse static model, the physical variables can be averaged to give values at the centers of the zones. This rezoning, however, does not provide a model in exact hydrostatic and thermal equilibrium. Initiation of the pulsation code with such a model is found to lead to violent instabilities, whose decay in the interior zones is extremely slow. For this reason, the model has to be again set in full equilibrium by using a differencing scheme consistent with the pulsation code. The final model obtained in this way constitutes the initial model for the pulsational study.

#### b) *The Dynamical Models*

The partial differential equations of stellar pulsation have been cast into finite-difference form with mass as the independent space variable. A semi-implicit scheme described in detail by Christy (1964, 1967) has been used to set up and solve these difference equations.

For the numerical treatment of shocks, an artificial viscous pressure should be added to the difference equations. Stellingwerf's (1975) form of the viscosity has been adopted here, because this form does not introduce unwanted viscous damping in the interior (adiabatic) part of the model. In most of our models, the viscous coefficient  $C_v$  is set to 1.0 and the cutoff parameter  $\alpha$  to 0.1.

At large pulsational amplitudes, the physical variables in the outer zones change very rapidly during certain phases. Therefore, the use of the Courant condition to determine the size of the time step during these phases often leads to too large a predicted temperature change. Since the temperature of each zone must be subsequently iterated to a chosen accuracy of one part in  $4 \times 10^6$ , it may happen that the iterations fail to converge, and often they diverge violently. In such circumstances the time step is cut down by a specified factor and the iteration procedure is reinitiated. This process can be repeated if an even smaller time step seems to be required. Another instance when the time step is arbitrarily cut down occurs in the event that the number of iterations exceeds a specified limit of 10. However, the normal number of iterations required is less than six. For one pulsation cycle, the number of time steps used is typically about 300.

The period is determined by ascertaining when the radius of a selected zone returns to its initial value. For this purpose, a relatively deep zone is chosen where the cyclical variation of the radius is smooth and nearly sinusoidal. At the end of a period, the other physical variables generally do not return to *exactly* their initial values, because small numerical errors have unavoidably been incurred during computation. Therefore the computed  $\int PdV$  work done by each zone over a period shows random fluctuations from cycle to cycle. In order to exactly close the loop integral, we have added the quantity  $0.5(P_{\text{initial}} + P_{\text{final}})(V_{\text{initial}} - V_{\text{final}})$  to the approximately computed value of  $\int PdV$ .

The limiting amplitude of pulsationally unstable models can be reached by starting from either (a) the white noise of the initial equilibrium model or (b) a suitable choice of an initial velocity distribution, such as an assumed power-law dependence on  $r/R$  or else an arbitrary scaling of the velocity distribution obtained from linearized pulsation theory. We have selected method (b) with a power-law dependence. The power law has been adapted from Stobie's (1969a) formulae when available or else determined by trial and error so that the dispersion of the velocity amplitudes during the first six periods is small. To attain limiting amplitude in a reasonable expenditure of computer time, the velocity of each zone has been amplified after a lapse of three to six periods by a factor ranging from 1.4 to 1.1, depending on the nearness of the model to limiting amplitude. In order not to disturb the model structure too much, the boost in velocity amplitude is provided at the phase of peak kinetic energy when the envelope is expanding most rapidly. After the model has nearly reached

limiting amplitude, as defined by a nearly constant peak kinetic energy, an additional amplification is given to see if the peak kinetic energy comes back down to the correct limiting value. This method ensures that limiting amplitude has truly been reached, a condition that may otherwise be masked in cases where the growth rate is very slow. At this amplitude, the model is run for several periods to remove the presence of any unwanted modes. The period and the surface velocity curve must then have attained an exactly repeating behavior. In our work, the term "surface" will be taken to mean the layer at which the optical depth of the static model was about 0.2.

After the numerical adjustment of the original static model and the initiation of pulsations, the mean luminosity and effective temperature of the star are no longer precisely the equilibrium values. However, we shall ignore these very small differences and refer to the models in terms of their equilibrium luminosities and effective temperatures.

### III. TESTS OF THE PROGRAM

In order to check the computer code, we have recalculated two Cepheid models that have been previously calculated by other authors:

(1) Goddard model:  $M/M_{\odot} = 4$ ,  $\log(L/L_{\odot}) = 3.503$ ,  $\log T_e = 3.756$ ,  $X = 0.700$ ,  $Z = 0.020$ , Los Alamos opacities (Castor *et al.* 1976).

(2) Christy model 5gF:  $M/M_{\odot} = 0.578$ ,  $\log(L/L_{\odot}) = 1.585$ ,  $\log T_e = 3.813$ ,  $X = 0.698$ ,  $Z = 0.002$ , Los Alamos opacities (Christy 1966).

In each case we have used Christy's (1966) analytic fit to the earlier Los Alamos opacities and approximately the same number of mass zones, time steps, etc., as did the previous authors, except that we have adopted Stellingwerf's form of the artificial viscosity for the Goddard model. Our results are found to be in very good agreement with previous ones. Details of our version of the Goddard model are presented in Figure 1 and immediately below, for comparison with the set of models computed by several other authors (Castor *et al.* 1976):

Zones optically thin	52/5
Viscosity	1S.10
Number of periods calculated	30
Number of time steps per period	350
$r_1/R$	0.089
Period (days)	$9.75 \pm 0.03$
Method	Radius crossing
Growth rate	8.3% K.E.
K.E. ( $10^{42}$ ergs)	2.4
Machine	360/95
Periods per minute	0.5

The fact that our peak kinetic energy is somewhat higher than the values obtained by other authors suggests either that their models may not have achieved limiting amplitude or that the difference in opacity representation is causing the variation.

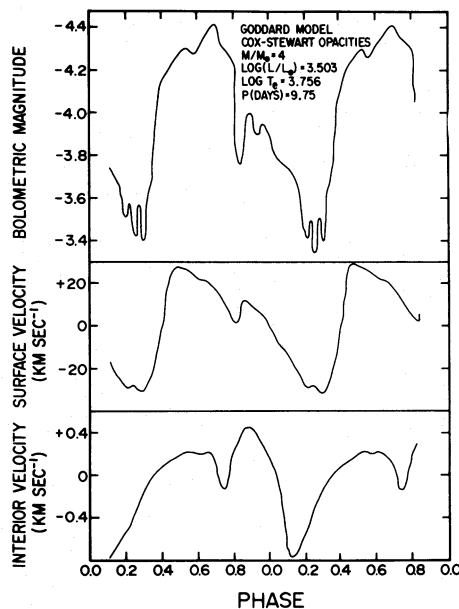


FIG. 1.—The Goddard model, calculated with Cox-Stewart opacities. The surface luminosity and surface velocity curves refer to optical depth  $\sim 0.2$  of the static model. The interior velocity curve refers to a layer with a temperature of  $\sim 2 \times 10^5$  K in the static model.

If the Goddard model is computed with Carson's opacities, the result is markedly different. In this case, RV Tauri behavior is exhibited (§ IV). In the case of the Cox-Stewart opacities, such behavior occurs only at much higher  $R/M$  ratios (Stobie 1969*b*; Christy 1975).

### IV. NEW NONLINEAR RESULTS

To reproduce the observed bump Cepheids, stellar masses must be used that range from values expected from normal evolutionary theory without mass loss to as small values as seem to be required to produce "bumps" on the luminosity and velocity curves. The observed luminosities and effective temperatures, though somewhat uncertain, probably lie within the ranges  $3.5 \leq \log(L/L_{\odot}) \leq 3.7$  and  $3.75 \leq \log T_e \leq 3.81$  (Fricke, Stobie, and Strittmatter 1972). Therefore, the expected masses are 6–8  $M_{\odot}$ , if the bump Cepheids are evolving in the slow "blue loop" phase of core helium burning; the much less likely hypothesis that they are in the rapid "first crossing" phase of core helium ignition leads to expected masses of 7–9  $M_{\odot}$ .

Our adopted grid of theoretical models is listed in Table 1, together with a summary of our main results. In this table, notation is conventional, but we mention explicitly the following quantities for definiteness: K.E., peak kinetic energy;  $\Delta$ , full (not half) amplitude; *Asymmetry*, time spent on the descending branch of the surface velocity curve divided by time spent on the ascending branch;  $\phi$ , phase after zero velocity at minimum radius of the second (but not

TABLE 1  
FULL-AMPLITUDE PROPERTIES OF THE MODELS WITH  $Y = 0.24$

$M/M_{\odot}$	$\log(L/L_{\odot})$	$\log T_{\ast}$	$R/R_{\odot}$	$P$ (days)	K.E. ( $10^{42}$ ergs)	$\Delta R/R$	$V_{\text{out}}$ ( $\text{km s}^{-1}$ )	$V_{\text{in}}$ ( $\text{km s}^{-1}$ )	$\Delta V$ ( $\text{km s}^{-1}$ )	$L_{\text{max}}$ ( $10^{37}$ ergs $\text{s}^{-1}$ )	$L_{\text{min}}$ ( $10^{37}$ ergs $\text{s}^{-1}$ )	$\Delta M_{\text{bol}}$	Asym- metry	$\phi$	$\delta\phi$	Bump	$P_{3}/P_0$
4	3.5	3.75	60.2	11.35	4.3	0.32	46	-41	87	3.5	0.45	2.2	1.2	1.27	0.27	A*	0.488:
				11.45	4.0	0.32	50	-64	114	1.8	0.20	2.4	3.2	...	0.10	X*	0.488:
5	3.5	3.75	60.1	9.51	3.1	0.20	28	-41	69	1.8	0.49	1.4	4.8	1.47	0.08	D	0.517
				7.44	3.9	0.18	38	-53	91	1.8	0.50	1.4	6.7	1.60	0.10	D	0.536
				5.82	2.1	0.15	34	-33	67	1.8	0.70	1.0	4.0	1.54	0.09	D	0.551
5	3.7	3.75	75.8	15.10	7.7	0.31	48	-35	82	5.8	0.30	3.2	1.5	1.28	0.28	A*	0.483:
				14.50	7.6	0.35	47	-65	112	2.9	0.30	2.5	2.9	...	0.09	X*	0.483:
				11.46	3.5	0.26	37	-42	79	3.5	1.1	1.3	1.2	1.31	0.31	A	0.508
				8.83	1.8	0.17	28	-31	59	2.8	1.3	0.8	2.7	1.46	0.07	D	0.529
6.4	3.5	3.78	60.7	7.74	5.5	0.19	42	-40	82	2.0	0.52	1.5	12.4	...	0.08	X	0.546
7	3.5	3.66	91.0	15.23	14.9	0.26	47	-49	96	2.5	0.24	2.5	1.6	1.26	0.26	A	0.491
				11.83	14.9	0.20	40	-52	92	2.2	0.13	3.1	5.5	1.50	0.11	D	0.512
				9.38	11.8	0.18	33	-48	82	1.7	0.15	2.6	4.6	1.57	0.10	D	0.539
				7.39	13.7	0.19	48	-53	101	1.9	0.36	1.8	7.8	1.77	0.07	XD	0.556
				5.77	11.4	0.19	45	-58	103	3.2	0.60	1.8	5.2	1.77	0.10	XD	0.567
				4.62	3.9	0.10	32	-27	59	1.8	0.70	1.0	2.9	1.58	0.10	XD	0.573
7	3.7	3.72	86.9	14.30	8.0	0.22	37	-43	80	3.1	0.65	1.7	1.5	1.33	0.33	A	0.505
				11.21	10.3	0.21	38	-50	88	2.8	0.66	1.6	4.8	1.52	0.10	D	0.527
				8.72	8.7	0.19	45	-48	93	3.6	0.86	1.6	4.1	1.59	0.09	D	0.543
				6.85	4.5	0.13	38	-32	70	2.7	1.3	0.8	3.8	1.64	0.09	XD	0.556
9	3.7	3.75	75.6	9.27	22.1	0.19	43	-53	96	2.8	0.68	1.5	5.3	1.69	0.08	D	0.556
				7.35	20.2	0.18	50	-47	97	3.4	0.72	1.7	6.0	1.70	0.09	XD	0.565
				5.80	1.8	0.05	14	-14	28	2.3	1.6	0.4	2.5	...	0.19	X	0.570
9	4.0	3.75	106.9	17.63	11.6	0.22	34	-40	74	6.1	1.8	1.3	1.0	1.36	0.36	A	0.509
				13.69	10.3	0.17	33	-41	74	5.4	2.3	0.9	4.4	1.51	0.10	D	0.528
				10.73	7.4	0.14	32	-29	61	5.2	2.6	0.8	2.4	1.54	0.11	D	0.542
11	4.3	3.75	147.2	30.23	67.5	0.42	54	-58	112	13.4	2.5	1.8	5.1	1.87	0.10	X†	0.488

\* RV Tauri-like behavior.

† An inflection in the surface velocity curve appears around minimum velocity.

necessarily the secondary) bump in the surface velocity curve plus unity;  $\delta\phi$ , phase of the surface velocity maximum minus phase of the surface radius minimum;  $P_2/P_0$ , ratio of the period of the second overtone to the period of the fundamental mode (derived from linear nonadiabatic theory). Under the heading *Bump*, the letter A stands for the presence of a secondary bump on the ascending branch of the surface velocity curve, while the letter D refers to a bump on the descending branch. If there is no bump, the letter X is used. Luminosity curves are not used for this purpose because, as is generally found, the luminosities near the surface tend to be noisy unless a fine zoning of the outer layers (including the hydrogen ionization zone) is adopted.

#### a) Work Curve

As a prototype bump Cepheid, we select one of our models characterized by  $M = 7 M_\odot$ ,  $\log(L/L_\odot) = 3.7$ ,  $\log T_e = 3.78$ , and  $P = 8.7$  days. The integrated work done over a pulsation cycle by each zone in this model is shown in Figure 2. Notice that pulsational driving occurs both in the helium ionization region (zones 27–34) and in the hydrogen ionization region (zones 34–44). In some of our models, the driving peak in the latter region is split into two subpeaks (a phenomenon discussed by Stellingwerf 1976). Very rarely, the helium peak is also partially split. It should be noted that no significant excitation or damping occurs in layers with temperatures higher than  $\log T = 5.4$  (zone 10); therefore, the large CNO opacities that Carson derived for such high temperatures have no effect on the pulsational properties of the models.

#### b) Velocity Curves

Velocity curves for our prototype model are shown in Figure 3. A magnified scale is used to plot velocities in the lower zones so that the small structure becomes visible. It will be noticed that Christy's (1968) "echo" phenomenon can be traced in our models. Thus, a running wave is propagated inward from the helium

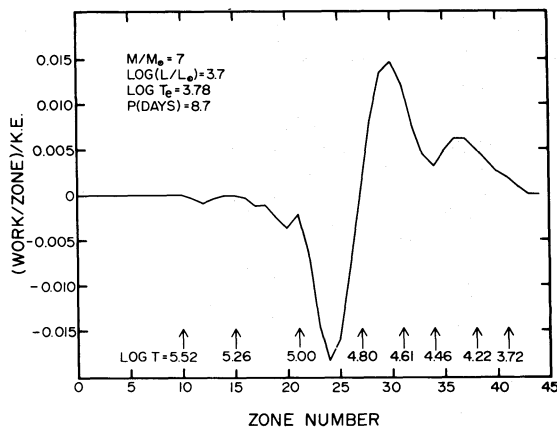


FIG. 2.—Work integral per zone, in units of the peak kinetic energy, for a model of  $7 M_\odot$  at limiting amplitude. The temperatures of a few zones in the static model are indicated.

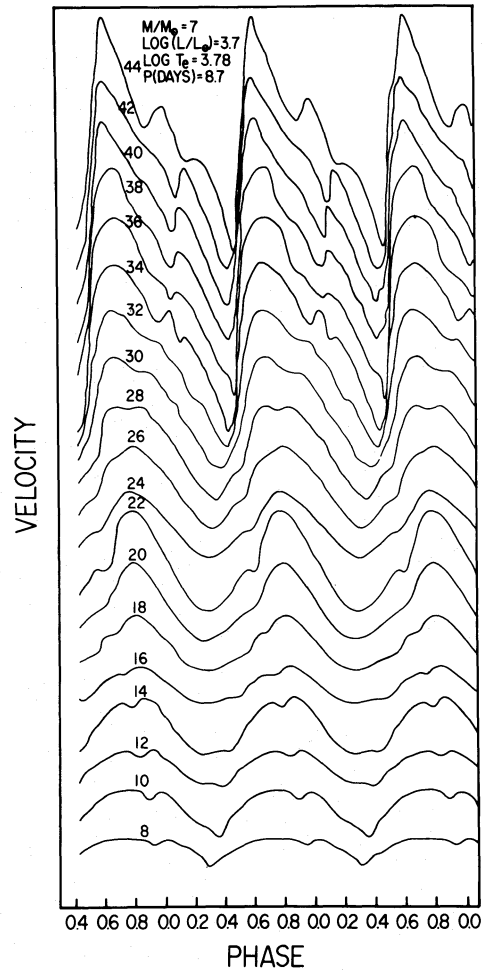


FIG. 3.—Velocity curves for various zones in a model of  $7 M_\odot$ . The zone numbers are indicated. The vertical scale is different for the various zones.

ionization region (starting from near zone 28) and is then reflected off the central core; eventually the wave arrives at the surface about 1.6 periods after its initiation. This disturbance at the surface causes a secondary bump to appear on the descending branch of the velocity curve (zone 40). The primary bump in this curve seems to be due to the arrival of the running wave that is propagated directly outward from the helium ionization region at the same time as the inward-wave is initiated. For comparison, the velocity curves for a model of  $5 M_\odot$  with the same luminosity and effective temperature as those of the prototype are shown in Figure 4. The period of this model is significantly longer (11.5 days), and the secondary bump now appears on the ascending branch of the velocity curve (zone 30).

It is well known from Stobie's (1969*b, c*) and Christy's (1975) work that the observed (Ledoux and Walraven 1958) progression of the shape of the light and velocity curves with increasing period can be qualitatively reproduced by theoretical nonlinear

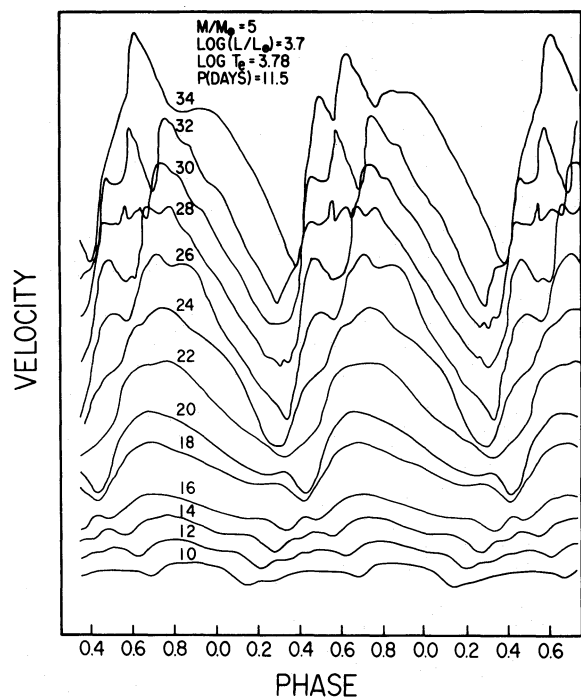


FIG. 4.—Velocity curves for various zones in a model of  $5 M_{\odot}$ . The zone numbers are indicated. The vertical scale is different for the various zones.

models. Our quantitative results for  $M = 7 M_{\odot}$  and  $\log(L/L_{\odot}) = 3.7$ , based on the new opacities, are shown in Figures 5 and 6. Three main features of the velocity curves, which are more accurately determined than the luminosity curves, should be noted. First, the phase of maximum outward velocity occurs very close to the phase of maximum luminosity, as is actually observed (although there are differences in detail). Second, a small bump appears initially on the descending branch of the velocity curve around a period of 7 days, then grows and progresses forward with respect to velocity minimum until it switches to the ascending branch around a period of 12 days. Observationally, the corresponding periods are about 7 and 10 days. Third, the models predict a large asymmetry in the surface velocity curve when the amplitude is high, and a small asymmetry when the amplitude is low. This correlation is in fact observationally corroborated. The theoretical and observed values of the asymmetry are  $\sim 4$  for velocity curves that have a bump on the descending branch, and  $\sim 1$  for velocity curves that have a bump on the ascending branch. The *average* surface velocity amplitudes predicted by the models are roughly  $80 \text{ km s}^{-1}$ . In comparison, the average empirical velocity amplitudes, formed by multiplying the observed radial-velocity amplitudes by  $24/17$ , are only about  $60 \text{ km s}^{-1}$ . However, the discrepancy seems small in view of the crude treatment of the outer layers in our models. All the foregoing conclusions are equally valid for any other reasonable choice of stellar mass and luminosity (see the full results in Table 1).

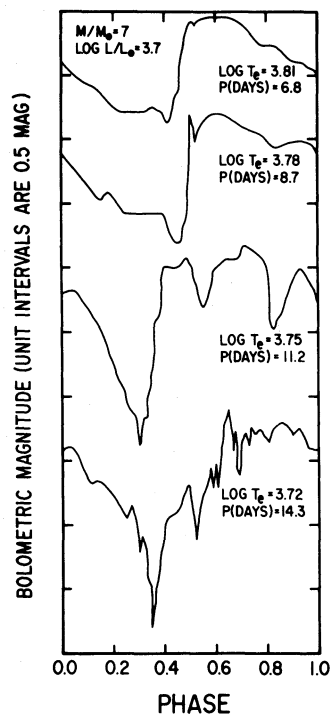


FIG. 5.—Progression of the surface luminosity curves with period for selected models of  $7 M_{\odot}$ .

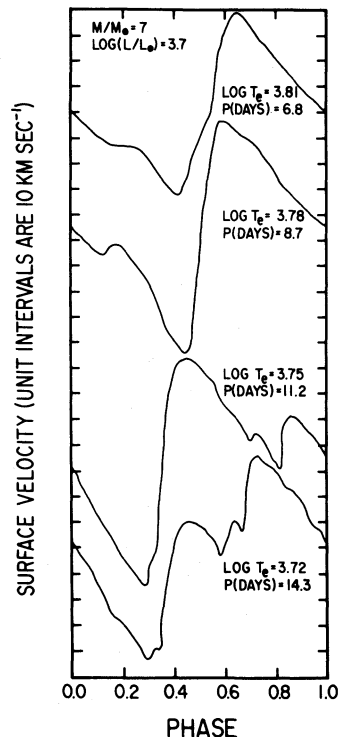


FIG. 6.—Progression of the surface velocity curves with period for selected models of  $7 M_{\odot}$ . Compare Fig. 5.

Another, indirect measure of the asymmetry of the surface velocity curve is given by  $\delta\phi$ . Its theoretically predicted increase with period is confirmed very elegantly by the recent observational data of Evans (1976). A further point of agreement with observation is the lack of a prominent secondary bump at very long periods (see our model for  $P = 30.2$  days) and, occasionally, at periods where a bump is the rule (see our models in the period range 5.8–7.7 days). It should be emphasized that, in any sequence of models in which two of the parameters (mass, luminosity, effective temperature) are held fixed, the progression of the bump is smooth and unbroken; but the periods at which the bump is first and last visible are not the same for every sequence. Since Cepheids of the same luminosity and effective temperature could have at least three different implied masses (corresponding to the three different evolutionary crossings of the instability strip), there could be a small range of periods where Cepheids with and without bumps coexist. The assumption that not all Cepheids have the same initial chemical composition could introduce additional scatter.

### c) Masses of Bump Cepheids

Fricke, Stobie, and Strittmatter (1972) have shown that, if one defines  $\phi$  in the manner indicated above, then the product  $P\phi$  turns out to be nearly proportional to the radius  $R$ . This result was already implicit in the earlier work of Christy (1968, 1970), Stobie (1969*b, c*), and Fricke, Stobie, and Strittmatter (1971). More recently, Christy (1975) has confirmed and

interpreted it in terms of his echo concept. With Carson's opacities, we find:

$$P\phi \approx 0.22(R/R_{\odot}) \text{ days}, \quad (1)$$

with a range of scatter in the coefficient of  $\pm 0.03$ .

Another useful quantity is the "pulsation constant,"

$$Q = P(M/M_{\odot})^{1/2}(R/R_{\odot})^{-3/2}. \quad (2)$$

This is not exactly a constant but is approximately proportional to  $(R/M)^{1/4}$  for a wide range of stellar models. With Carson's opacities, we find:

$$P \approx 0.025(R/R_{\odot})^{7/4}(M/M_{\odot})^{-3/4} \text{ days}, \quad (3)$$

where the coefficient has a scatter of  $\pm 0.001$ .

By combining the  $(P, \phi, R)$  and  $(P, \bar{M}, R)$  relations, it is possible to obtain a formula for the mass of a bump Cepheid in terms of the directly observable parameters  $P$  and  $\phi$ . With Carson's opacities,

$$M/M_{\odot} \approx 0.25P\phi^{7/13}. \quad (4)$$

Since observed bump Cepheids have  $\langle P \rangle = 8$  days and  $\langle \phi \rangle = 1.6$  (Fricke, Stobie, and Strittmatter 1972), we may infer that they have an average mass of  $\langle M/M_{\odot} \rangle \approx 6.0$ . The situation is illustrated in detail in Figure 7, where individual bump Cepheids are plotted along with the individual theoretical models. It is worth noting that more of the stars should have a bump on the descending branch if the average mass is greater than  $6 M_{\odot}$ , but more should have one on the ascending branch if the average mass is smaller than  $6 M_{\odot}$ .

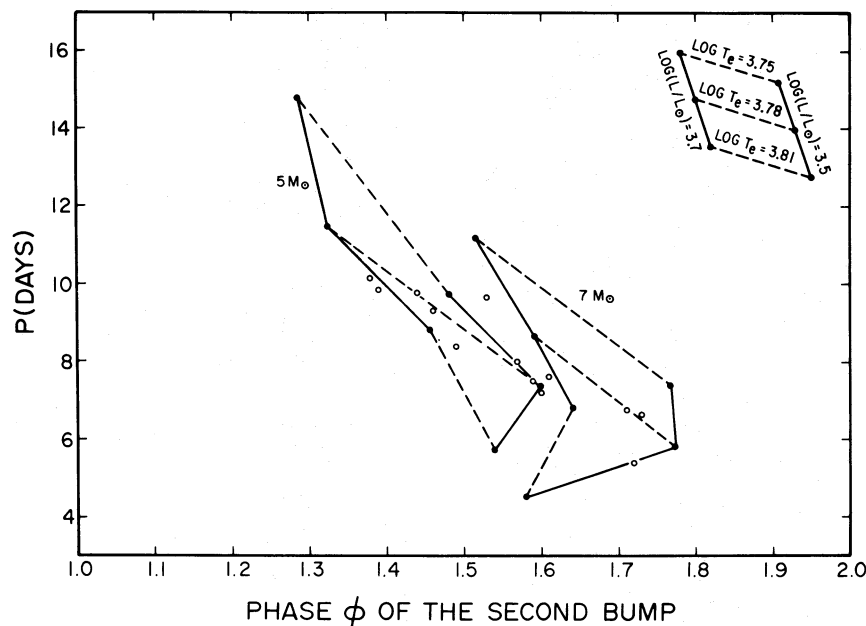


FIG. 7.—Relation between the period and the phase of the second bump on the surface velocity curve, for the theoretical models (filled circles) and for observed bump Cepheids (open circles). The grid connecting the theoretical models of a fixed mass is explained schematically in the upper right corner.

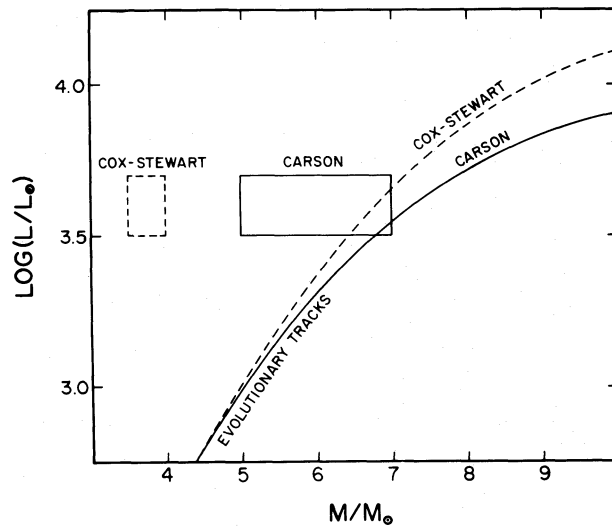


FIG. 8.—Mass-luminosity diagram both for bump Cepheids (boxes) and for stellar models that have evolved to the “second crossing” phase without mass loss (curves). The results for the two adopted sets of opacities are shown.

Previous authors have obtained  $\langle M/M_{\odot} \rangle \approx 3.8$  with the use of the Cox-Stewart opacities. The difference from our results is striking. Only a small part of this difference can be due to the slightly different choices of chemical composition (see Fricke, Stobie, and Strittmatter 1971). About 30% of the difference actually comes from the change of the  $Q$  value (Carson and Stothers 1976); but by far the greater percentage arises from the change of  $\phi$ .

To effect a further comparison, the regions of the mass-luminosity plane occupied by bump Cepheids are shown for the two sets of opacities in Figure 8. Also shown are the corresponding evolutionary mass-luminosity relations for stellar models that have evolved to the “blue loop” phase without mass loss. The evolutionary mass-luminosity relation for  $M/M_{\odot} > 8$  in the case of Carson’s opacities is extrapolated, since a “blue loop” does not occur at such high masses with his opacities if  $Z \geq 0.02$  (Stothers and Chin 1978). The small differences in luminosity that result from switching from one set of opacities to the other are caused mainly by the differences in the contributions to the total opacity coming from the CNO elements at temperatures of  $\log T = 5.4$ – $6.4$ .

We regard Figure 8 as important evidence that Carson’s opacities (for at least the element helium) may be superior to those of the Los Alamos group. A small improvement in Carson’s opacities could possibly bring the pulsational masses of bump Cepheids into perfect agreement with the evolutionary masses. Alternatively, since the red-giant precursors of Cepheids are observed to be losing mass, an average 15% loss of a red giant’s initial mass could be invoked to achieve exact agreement. However, it is known from evolutionary calculations that a loss of between 10% and 80% of a star’s initial mass will completely suppress the “blue loop.” This result has been ob-

tained both for the Cox-Stewart opacities (Forbes 1968; Lauterborn, Refsdal, and Weigert 1971) and for Carson’s opacities (Stothers and Chin 1978). Nevertheless, the model uncertainties are such that they probably do not entirely preclude a mass loss of 15%. An affiliated problem is that the empirical mass-loss rates, as recently calibrated by Reimers (1977), are about 50 times too small to yield the necessary amount of mass loss. However, these “observed” rates are stated by Reimers to be only lower limits to the true rates. In fact, Bernat’s (1977) rates are between one and two orders of magnitude higher than Reimers’s.

It is worth recalling that Carson and Stothers (1976) have found pulsational masses of Cepheids based on the  $(P, M, R)$  relation to be almost as low with Carson’s opacities as they are with the Cox-Stewart opacities. Using radii determined from the observed luminosities and effective temperatures of bump Cepheids (Fricke, Stobie, and Strittmatter 1972), we find specifically that, if  $\langle P \rangle = 8$  days and  $\langle R/R_{\odot} \rangle = 55$ , the average mass according to equation (3) is  $\langle M/M_{\odot} \rangle \approx 5.3$ . If the accepted absolute magnitudes of Cepheids were brighter by 0.11 mag or if their accepted effective temperatures were 3% cooler, their average mass could be made equal to 6.0. This uncertainty is probably permitted by the observational errors.

#### d) Change of Helium Abundance

To test the effect of a uniform change in the chemical composition of the stellar envelope, we have recalculated the two models shown in Figures 3 and 4 with new composition parameters  $(X, Y, Z) = (0.49, 0.49, 0.02)$ . Only the helium abundance is of interest here since the metals abundance has a relatively small effect on the pulsational properties. Following Fricke, Stobie, and Strittmatter (1971), we may express our results (which are given in detail in Table 2) as a relationship between the helium abundance and the stellar mass inferred from  $P$  and  $\phi$ . It is found, from the two models for  $7 M_{\odot}$ , that  $M \propto Y^{-0.2}$  while, from the two models for  $5 M_{\odot}$ ,  $M \propto Y^{-0.4}$ . By using the Cox-Stewart opacities, Fricke, Stobie, and Strittmatter (1971) found  $M \propto Y^{-0.39}$ . Apparently, the exponent is not very sensitive to the adopted set of opacities.

It is of interest to ascertain whether, with a given set of opacities, the change in the inferred mass is due to the change in mean molecular weight or to the change in opacity, since both factors depend on  $Y$ . Therefore, we have taken the original model for  $7 M_{\odot}$  and have introduced the new composition parameters  $(X, Y, Z) = (0.49, 0.49, 0.02)$  into the thermodynamic state variables, while retaining the original-composition opacity tables. Our results, shown in Table 2, indicate that  $P$  is affected about equally (though in opposite directions) by the two factors—mean molecular weight and opacity—and that  $\phi$  is considerably more sensitive to mean molecular weight than to opacity (but again the two factors act in opposite senses).

TABLE 2  
FULL-AMPLITUDE PROPERTIES OF THE MODELS WITH VARIOUS HELIUM ABUNDANCES

PARAMETER	$M/M_{\odot} = 5$		$M/M_{\odot} = 7$		
	0.24*, 0.24†	0.49*, 0.49†	0.24*, 0.24†	0.49*, 0.49†	0.49*, 0.24†
$R/R_{\odot}$ .....	66.0	65.9	65.9	65.8	65.8
$P$ (days).....	11.46	11.50	8.72	8.69	8.59
K.E. ( $10^{42}$ ergs).....	3.5	4.2	8.7	19.0	13.8
$\Delta R/R$ .....	0.26	0.21	0.19	0.19	0.19
$V_{\text{out}}$ ( $\text{km s}^{-1}$ ).....	37	30	45	45	47
$V_{\text{in}}$ ( $\text{km s}^{-1}$ ).....	-42	-39	-48	-60	-53
$\Delta V$ ( $\text{km s}^{-1}$ ).....	79	69	93	105	100
$L_{\text{max}}$ ( $10^{37}$ ergs $\text{s}^{-1}$ ).....	3.5	2.9	3.6	3.0	3.3
$L_{\text{min}}$ ( $10^{37}$ ergs $\text{s}^{-1}$ ).....	1.1	0.87	0.86	0.27	0.57
$\Delta M_{\text{bol}}$ .....	1.3	1.3	1.6	2.6	1.9
Asymmetry.....	1.2	5.3	4.1	8.2	6.6
$\phi$ .....	1.31	1.51	1.59	1.68	1.72
$\delta\phi$ .....	0.31	0.10	0.09	0.11	0.08
Bump.....	A	D	D	D	D

\*  $Y$  for state.

†  $Y$  for opacity.

NOTE.—In both the  $M/M_{\odot} = 5$  and  $M/M_{\odot} = 7$  cases, we have used  $\log(L/L_{\odot}) = 3.7$  and  $\log T_{\text{e}} = 3.78$ .

#### V. NEW LINEAR RESULTS

##### a) The Resonance $P_2/P_0 = 0.5$

Second-overtone periods have been calculated for the models of Table 1 by employing linear non-adiabatic theory. The computer program adopted is that of Carson and Stothers (1976). It is basically compatible with the nonlinear program that we have written, except that the surface boundary condition for the heat flow is somewhat different. However, this small difference is not expected to affect the periods significantly. Since Cox, Hodson, and King (1978) have shown generally that linear and large-amplitude nonlinear periods agree closely with each other, our period ratios should be well determined even for large-amplitude pulsators.

Our interest in this section focuses on the ratio of the second-overtone period to the fundamental period ( $P_2/P_0$ ). Simon and Schmidt (1976) and Simon (1977) have argued that an accidental resonance, occurring when  $P_2/P_0 = 0.5$ , causes the excited fundamental mode to pick up the second overtone; the consequently modulated light and velocity curves are expected to show a bump on the ascending (A) or the descending (D) branch, depending on which side of the resonance the period ratio lies. By matching Stobie's (1969*b, c*) theoretical velocity curves, their own linearized period ratios, and observational data for bump Cepheids, Simon and Schmidt have derived bump masses of about half the evolutionary masses with resonance limits of  $P_2/P_0 = 0.46$ – $0.48$  (A models) and  $P_2/P_0 = 0.50$ – $0.53$  (D models).

There seem to be several difficulties with this theory. First of all, a forced second-overtone oscillation is hard to reconcile with Christy's echo concept, which seems to explain very well the behavior of the velocities. Second, some of Stobie's models pulsating in the first overtone show a secondary bump on the

surface velocity curve. This bump for  $7 M_{\odot}$  and  $\log(L/L_{\odot}) = 3.7$  shifts from the descending branch to the ascending branch when the effective temperature of the star is decreased, just as it does in the case of the fundamental mode. But the first overtone is certainly not in resonance with the second (or even the third) overtone. Third, our models of bump Cepheids show  $P_2/P_0 = 0.48$ – $0.51$  (A models) and  $P_2/P_0 = 0.51$ – $0.56$  (D models). If the bumps are due to the supposed resonance, then the resonance limits are surprisingly wide and also are not symmetrical about  $P_2/P_0 = 0.50$ . As two examples, our prototype bump Cepheid model with  $P_2/P_0 = 0.543$  is shown in Figure 3, and a model for  $9 M_{\odot}$  with  $P_2/P_0 = 0.556$  is shown in Figure 9. Fourth, not all the models within the formal resonance limits have bumps (for an explanation see the analogous discussion at the end of § IV*b*). Our model for  $6.4 M_{\odot}$  with  $P_2/P_0 = 0.546$  does not show any sign of a bump, although it has a large amplitude.

A note of caution should be sounded in connection with the period ratios quoted by Simon and Schmidt. These were derived on the basis of linear adiabatic theory. However, nonadiabatic effects have a noticeable influence on the periods of the higher pulsation modes, because for these modes more of the pulsation amplitude is contained in layers closer to the surface. We find that nonadiabatic effects generally increase the period. Special calculations for models of  $7 M_{\odot}$  with  $\log(L/L_{\odot}) = 3.7$  indicate that, for both sets of opacities (Carson and Cox-Stewart), the difference between the nonadiabatic and adiabatic  $P_2/P_0$  values is  $0.015 \pm 0.001$ , i.e., essentially independent of  $P_0$ . Therefore, the addition of 0.015 to the resonance limits of  $P_2/P_0$  derived by Simon and Schmidt should correct them for nonadiabatic effects. The resulting limits turn out to be very close to the results that we have derived on the basis of Carson's opacities.

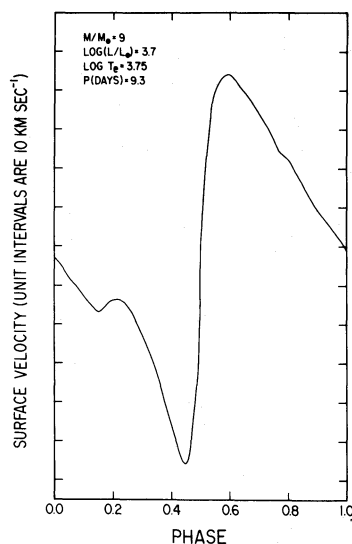


FIG. 9.—Surface velocity curve for a model of  $9 M_{\odot}$  with  $P_2/P_0 = 0.556$ .

#### b) Surface Phase Lag

The linearized calculations of Carson and Stothers (1976) have indicated that the phase lag (with respect to an adiabatic oscillator) between the luminosity variation and the radial-velocity variation at the stellar surface should be about  $45^\circ$  for stars that lie near the blue edge of the Cepheid instability strip and about  $135^\circ$  for very much redder stars. Convection, although it was included in the equilibrium structure of their stellar models, was not allowed to interact with the pulsations. By an obvious, but incorrect, interpolation, Carson and Stothers concluded that the average Cepheid ought to show a phase lag of about  $90^\circ$ , as is actually observed. However, by performing additional linearized calculations with similar physical assumptions, we have determined that the surface phase lag moves *clockwise* as the star moves redward across the instability strip. Therefore, the models including convection actually predict a phase lag of about  $270^\circ$  for the average Cepheid. On the other hand, with convection entirely omitted, the surface phase lag is found to move *counterclockwise* as the star moves redward, so that it reaches  $90^\circ$  where the average Cepheid lies. Since rather similar results have already been reported for models based on the Cox-Stewart opacities (Baker and Kippenhahn 1965; Castor 1971), it seems safe now to conclude that the phase lag must behave as if convection were absent. Therefore, our neglect of convection in the nonlinear models is probably justified.

#### c) Blue Edges

Our nonlinear computer program uses somewhat different surface boundary conditions from those used in the linear program of Carson and Stothers (1976). It would be useful to know what effect the different surface boundary conditions have on the predicted blue edges of the instability strip on the

H-R diagram. Since King *et al.* (1973) have shown generally that linear and nonlinear blue edges coincide, we have used our present computer program to re-determine the theoretical blue edges determined previously by Carson and Stothers. These edges, given in terms of  $\log T_e$ , turn out to be within  $\pm 0.005$  of the previous edges. Since the latter have already been shown to agree well with the general position of the observed blue edge, the present results seem to confirm this agreement.

#### VI. CONCLUSION

Nonlinear calculations of models for bump Cepheids have previously shown that most of the basic features of these stars are successfully reproduced by models having half the normal evolutionary masses, if the Los Alamos opacities are adopted. It is a remarkable circumstance that with the rather different Carson opacities these same features can be reproduced at least as well, and probably better since normal to nearly normal evolutionary masses with normal helium abundances are now called for. Because the observed rates of mass loss from the red-giant precursors of Cepheids appear to be very small, we believe that the use of Carson's opacities gives better agreement with observation. These opacities have the additional advantage of accounting in a better way for the general position (though not the slope) of the observed blue edge of the instability strip in the H-R diagram. However, other problems (such as the small observed period ratios of the double-mode Cepheids) remain for both sets of opacities, and radical remedies like those of Cox *et al.* (1977), and Cox, Michaud, and Hodson (1978) may turn out in the end to be justified in part.

It is worth noting that the hypothesis of a resonance between the fundamental mode and the second overtone, if applied to the present results for bump Cepheids, leads to a lopsided resonance band and a displaced resonance center as compared with the results presented by Simon and Schmidt (1976). Because of this fact and some other considerations, we wonder whether the resonance  $P_2/P_0 = 0.5$  is a good explanation for and indicator of a bump Cepheid.

It is a pleasure to acknowledge material support from T. R. Carson for the provision of his opacities, L. Wink for his help with the equation of state subroutine, and R. F. Stellingwerf for numerous programming hints. In addition, we thank A. N. Cox and A. L. Merts for informative telephone discussions of Cepheid and opacity modeling, and Norman Simon for discussions of his results concerning period ratios and for other helpful comments. S. K. Vemury thanks the National Academy of Sciences-National Research Council for the award of a Research Associateship at the Institute for Space Studies and Dr. Robert Jastrow for his hospitality at the Institute. He also wishes to thank A. N. Cox for extensive discussions during a brief visit to Los Alamos and for his cordiality at the Scientific Laboratory.

## REFERENCES

- Baker, N., and Kippenhahn, R. 1965, *Ap. J.*, **142**, 868.  
 Bernat, A. P. 1977, *Ap. J.*, **213**, 756.  
 Carson, T. R. 1976, *Ann. Rev. Astr. Ap.*, **14**, 95.  
 Carson, T. R., and Stothers, R. 1976, *Ap. J.*, **204**, 461.  
 Castor, J. I. 1971, *Ap. J.*, **166**, 109.  
 Castor, J. I., et al. 1976, in *Proceedings of the Solar and Stellar Pulsation Conference*, ed. A. N. Cox and R. G. Deupree (Los Alamos: Los Alamos Scientific Laboratory), p. 243.  
 Christy, R. F. 1964, *Rev. Mod. Phys.*, **36**, 555.  
 ———. 1966, *Ap. J.*, **144**, 108.  
 ———. 1967, in *Methods in Computational Physics*, ed. B. Alder (New York: Academic Press), Vol. 7, p. 191.  
 ———. 1968, *Quart. J.R.A.S.*, **9**, 13.  
 ———. 1970, *J.R.A.S. Canada*, **64**, 8.  
 ———. 1975, in *Cepheid Modeling*, ed. D. Fischel and W. M. Sparks (Washington: NASA), p. 85.  
 Cox, A. N. 1977, private communication.  
 Cox, A. N., Deupree, R. G., King, D. S., and Hodson, S. W. 1977, *Ap. J. (Letters)*, **214**, L127.  
 Cox, A. N., Hodson, S. W., and King, D. S. 1978, *Ap. J.*, **220**, 996.  
 Cox, A. N., Michaud, G., and Hodson, S. W. 1978, *Ap. J.*, **222**, 621.  
 Cox, A. N., and Stewart, J. N. 1965, *Ap. J. Suppl.*, **11**, 22.  
 Evans, N. R. 1976, *Ap. J. Suppl.*, **32**, 399.  
 Forbes, J. E. 1968, *Ap. J.*, **153**, 495.  
 Fricke, K., Stobie, R. S., and Strittmatter, P. A. 1971, *M.N.R.A.S.*, **154**, 23.  
 ———. 1972, *Ap. J.*, **171**, 593.  
 King, D. S., Cox, J. P., Eilers, D. D., and Davey, W. R. 1973, *Ap. J.*, **182**, 859.  
 Lauterborn, D., Refsdal, S., and Weigert, A. 1971, *Astr. Ap.*, **10**, 97.  
 Ledoux, P., and Walraven, T. 1958, in *Handbuch der Physik*, ed. S. Flügge (Berlin: Springer-Verlag), Vol. 51, p. 353.  
 Merts, A. L. 1977, private communication.  
 Reimers, D. 1977, *Astr. and Ap.*, **61**, 217.  
 Rodgers, A. W. 1970, *M.N.R.A.S.*, **151**, 133.  
 Simon, N. R. 1977, *Ap. J.*, **217**, 160.  
 Simon, N. R., and Schmidt, E. G. 1976, *Ap. J.*, **205**, 162.  
 Stellingwerf, R. F. 1975, *Ap. J.*, **195**, 441.  
 ———. 1976, in *Proceedings of the Solar and Stellar Pulsation Conference*, ed. A. N. Cox and R. G. Deupree (Los Alamos: Los Alamos Scientific Laboratory), p. 267.  
 Stobie, R. S. 1969a, *M.N.R.A.S.*, **144**, 461.  
 ———. 1969b, *M.N.R.A.S.*, **144**, 485.  
 ———. 1969c, *M.N.R.A.S.*, **144**, 511.  
 Stothers, R., and Chin, C.-w. 1978, *Ap. J.*, in press.  
 Vemury, S. K., and Stothers, R. 1977, *Bull. AAS*, **9**, 360.

RICHARD STOTHERS and SASTRI K. VEMURY: Institute for Space Studies, Goddard Space Flight Center, NASA, 2880 Broadway, New York, NY 10025